Amplifier

The 16 channel multipurpose amplifier from the laboratory was used to amplify the pressure gauge signal. The amplification on each channel and the output was adjusted to keep within the sampling range of WaveLab (±10 V). It was sometimes a problem to keep within the sampling range and a lower amplification was tested but this made interference a major part of the signal.

Wave recorder

The wave recorder is used to collect and amplify the signal from the wave transducers. The 10 channel wave recorder was used throughout the experiments.

Low-pass filter (8 Hz)

The sampled wave gauge signals were sent through a Low-pass filter before the data acquisition unit. This was done to remove interference and high frequencies as there at no point of the measurement were generated waves with a period lower than one second.

Data acquisition unit

The two data acquisition units were used to convert the analogue signals to a digital signal ready to be sampled by WaveLab on the connected computer.

C.5 Post processing of experimental results

The sampled data needs to be calibrated and filtered before the results are ready to be used. It is furthermore necessary to align the different samples to make the comparison of different samples easier and more precise. The following is a description of how and why the process was used.

C.5.1 Aligning and offset

Aligning all samples and channels

The sampling run between 80 and 100 seconds depending on the experiments and it takes approximately 40 seconds before the first wave hits the wall. Because of the way the equipment was arranged in the wave laboratory this time may vary with ±5 seconds depending on the wave properties and the time between the start of the sampling and the start of the wave generator.

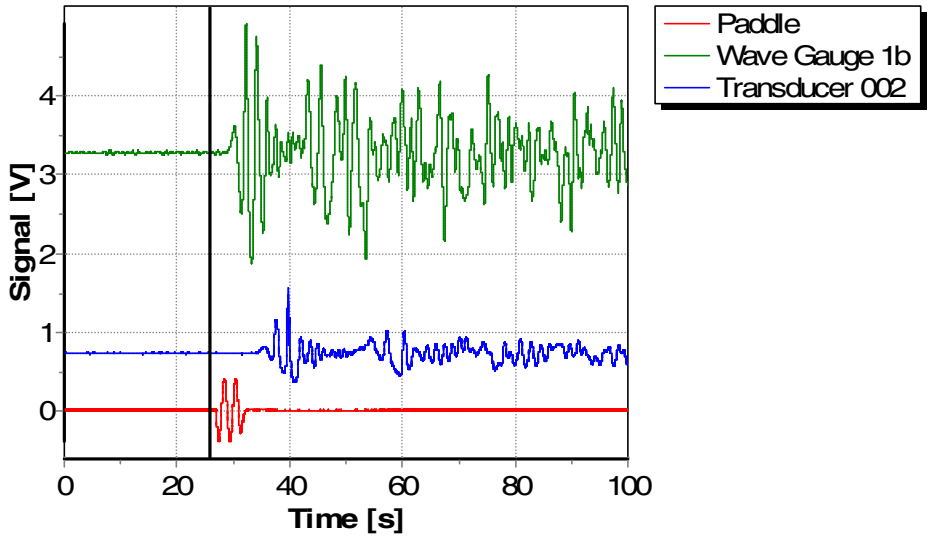

Figure C.12. This figure shows the three different signals from the same sample. The paddle starts the wave moment and the first detection of the movement is staggered down through the flume.

The first 23 seconds of the sample in Figure C.12 contains the time it takes to start the wave generation and the remaining time before Transducer 002 registers the first wave. The paddle movement is used in order to align the different samples and remove the superfluous start-up time. The paddle movement is chosen because it is identical for all the samples in the same series and it will always be the first thing to register movement.

Offset of pressure transducers

The aim of the experiments is to measure the change in pressure at the 16 pressure transducers as the original pressure is always known. In order to ease comparison of the pressure transducers the offsets of all the samples are centred at zero Volts as is depicted in Figure C.13 based on the last measurements of the sample.

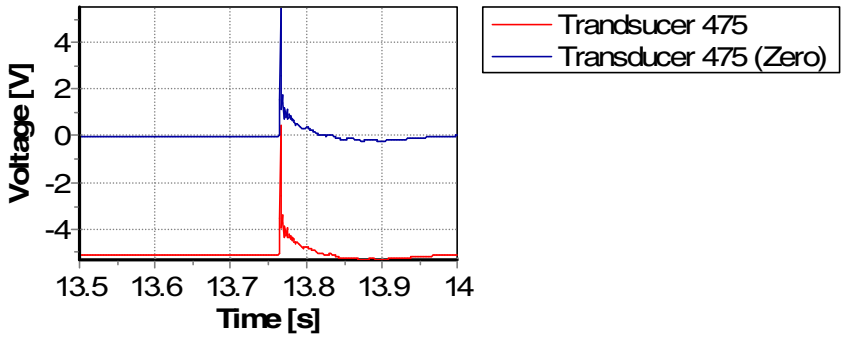

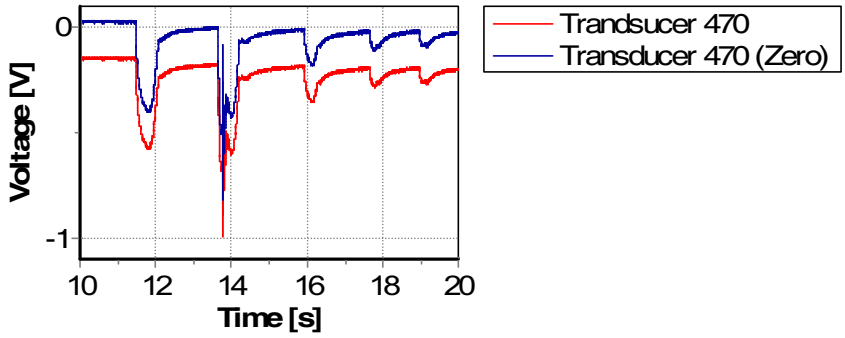

Figure C.13. On this figure it is depicted how the samples from transducer 470 (offset -0.17 V) and 475 (offset -5.11 V) are centred on zero. It is evident that transducer 470 has an initial offset when pressure is applied at 11 sec. Because of this the sample is centred on zero based on the last measurements of the sample.

C.5.2 Filtering

I was not necessary to apply any filter to the sampled time series as the interference was removed during measurement by choosing a higher amplification of the input signal. The interference was highest on the Ø8 transducers to such a degree that Transducer 479 was useless during Experiment no 1. The interference on the remaining transducers was satisfactory and a way was found to increase the amplification in subsequent experiments. It was not possible to remove the interference in the time series from Experiment no. 1. by using a filter as the noise interference was divided on several frequencies. This interference was clearly generated by the power grid and the connection.

C.5.3 Calibration

There are three types of measuring devices in this experiment and they are all calibrated differently. The description of how the different devices were calibrated and the resulting functions are listed on the following pages.

Wave gauges

The calibration of the wave gauges is done with the help of WaveLab before every third sample by changing the vertical position of the gauges with 0.1 m in still water. As the calibration is done every few experiments they are not all presented in the report. The exact calibration functions are available in the data files on the CD-ROM.

Paddle

The movement of the paddle is sampled as channel 10 and corresponding calibration function is shown in Figure C.14 and (C.1). The function was found by moving the paddle a known distance and registering the change in volt.

$$y = -0.2679x + 0.004 \tag{C.1}$$

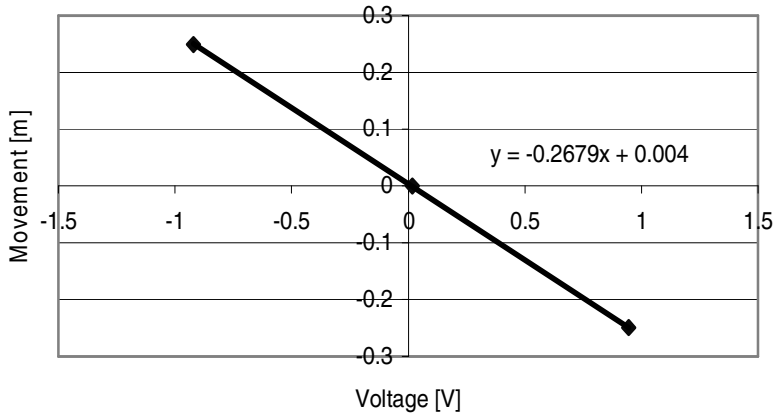

Figure C.14. Graph showing the measured relation between movement and current for the paddle and the corresponding linear tendency function.

Pressure transducers

The pressure transducers are organized into two rows AA and BB depending on their type. The transducers were calibrated by filling the flume and measuring the voltage at known levels of hydrostatic pressure. The depth at a given transducer was measured as defined in Figure C.15. The datum of the measurement is the original SWL displaced in Figure C.8 with h_{ini} = 0.25 m. This has no significance for the final use of the calibration functions as it is the fluctuations from the datum that are interesting and not the original level of pressure. Calibration was conducted in three runs (Calibration no. 1, 2 and 3) during which a great deal about liability of the transducers was discovered. The spreadsheet with all the calibration results is available on the CD-ROM.

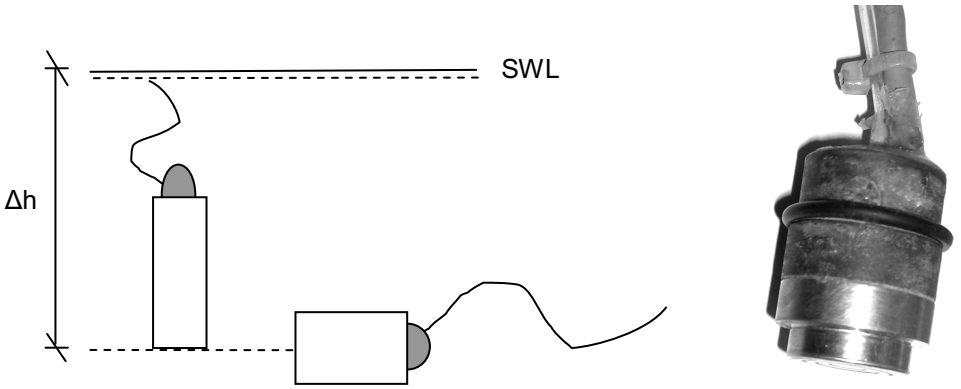

Figure C.15. On this figure it is depicted where the depth is measured depending on how the transducers are placed (vertical/horizontal). The picture to the right shows an example of a transducer in row AA.

The decision to make more than one sample was made when it was discovered that the offset of the transducers was slowly moving during the first week of experiments. The second round of calibration was made to investigate how it changed the measured voltage that the transducer had been subject to pressure. The third round of calibration was run as the last sample to ensure that the calibration had not changed during the last week of experiments. The series of water levels used in each calibration is presented in Figure C.16 and the results of calibration one and three are presented in Figure C.19 - Figure C.21.

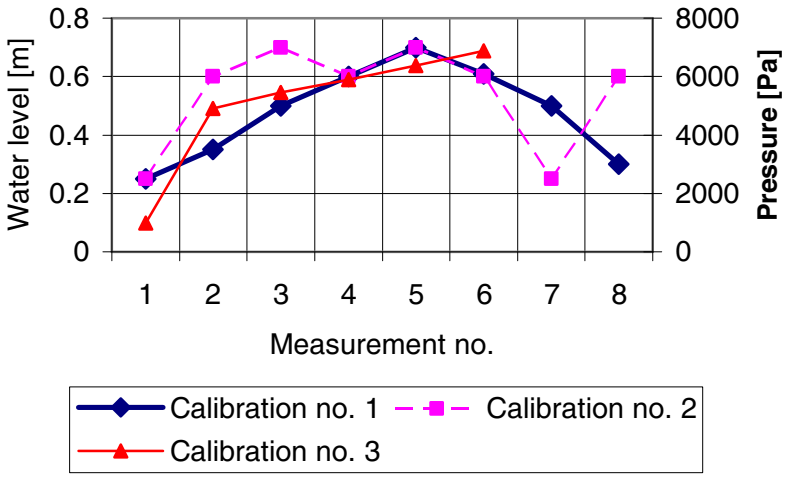

Figure C.16. Plot of the changing water level in and pressure at the bottom of the flume during the three calibrations the SWL is measured at the wall.

During all three calibration experiments the voltage at a given pressure was measured with a sampling frequency of 20 Hz. The used values are the mean of 20 sec long sample. No filtering has been used on these samples.

All the transducers installed in the wall were tested before installation to secure they had a relation between voltage and pressure that did not change if the transducers were left in the water a short period. This test disqualified most of the available transducers and only the best were used in the experiment.

It was discovered in calibration one and two that transducers in both rows were unstable. The transducers drifted when subjected to several changes in pressure especially the last comparison between two dry measurements could vary significantly as it is evident from Figure C.17. This could be caused by leaks in the transducers allowing water to change the relation between voltage and pressure especially because the first two calibrations were conducted over several hours giving the water plenty of time to exploit any weaknesses. The series of water levels are depicted in Figure C.16 and two examples of typical samples are presented in Figure C.17.

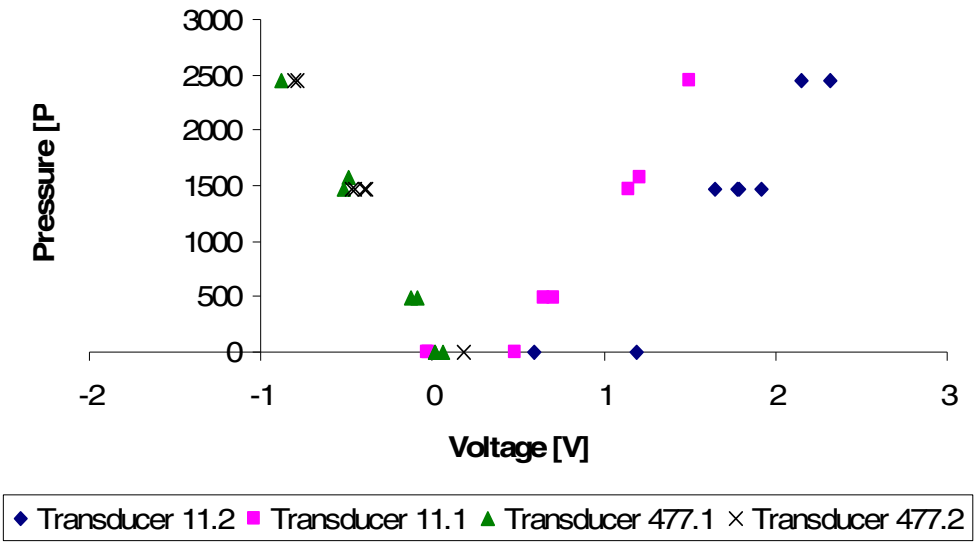

Figure C.17. A comparison between the samples from calibration no. 1 and 2 shows how a transducer measures a different voltage at the same pressure when the water level is changed several times up and down during the sample.

The samples depicted in Figure C.17 have a tendency to drift and although shown samples are among the worst it was nevertheless not feasible to use the functions from Calibration no. 1 and 2. Even if only the samples where all transducers was

submerged were used (water level > 0.45 m) it is evident that offset changed between the two calibrations and it was necessary to test if the relation between pressure and voltage was stable throughout the experiments.

A third calibration was devised to take place after finishing the experiments this time making it a priority to do the samples as fast as possible and have as many samples as possible with all the transducers submerged (water level > 0.45 m), cf. Figure C.16. The result is shown in Figure C.19 - Figure C.21 together with similar measurements from the first calibration. From these figures it is evident that only transducer 471 has experienced a radical change in the relation between voltage and pressure. The remaining transducers are relatively stable although the offset is changing and it must be noted that the offset of transducer 475 was changed manually on the amplifier to keep the sample within ±10V.

It was decided to use the third calibration and the corresponding functions listed in Table C.4. These functions were chosen because they are based on five points and all the measured pressures are taken while the transducers are submerged. By doing this the initial drift is taken into account and that is the big depicted difference in voltage at zero Pascal in Figure C.17. The drift taking place when the transducers are submerged is of lesser importance as measurements taken in the wave flume runs a maximum of two minutes with 15 minutes between each measurement.

It could have been a possibility to remove the transducers from the wall and calibrate them in a tube of water. This was not possible because of the tight fit between wall and transducers. This makes removal difficult and may damage/change the transducers.

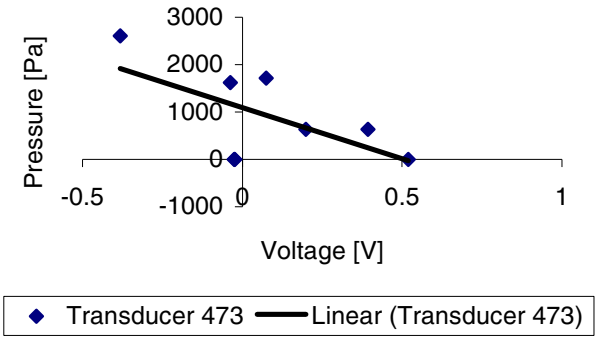

Figure C.18. On this figure the first calibration of transducer 473 is depicted. This transducer is the one with the greatest drift when changing the pressure level several times.

The results depicted in Figure C.19 - Figure C.21 show that transducer 471 is the only one with an inclination changing more than a few percent between calibration one and three. Special attention must also be directed at the results from the transducers 09, 11 and 471 as the second calibration shows that these transducers is the ones with the greatest drift during a calibration with several pressure levels. The worst is depicted in Figure C.18.

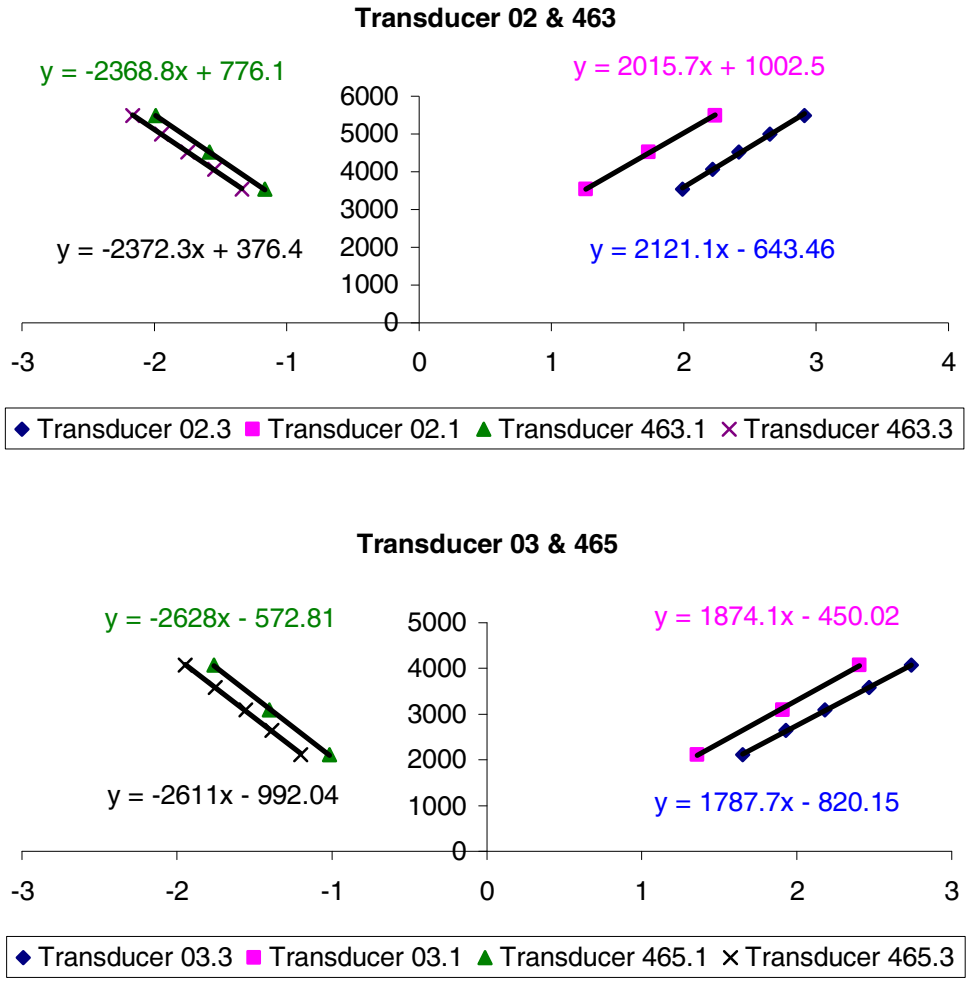

Figure C.19. Calibration functions for the first three rows of pressure transducers based on calibration one and three (Calibration on transducer 465 and calibration no. 3 is 465.3). Pressure is measured in Pa and voltage in volt (x-axis).

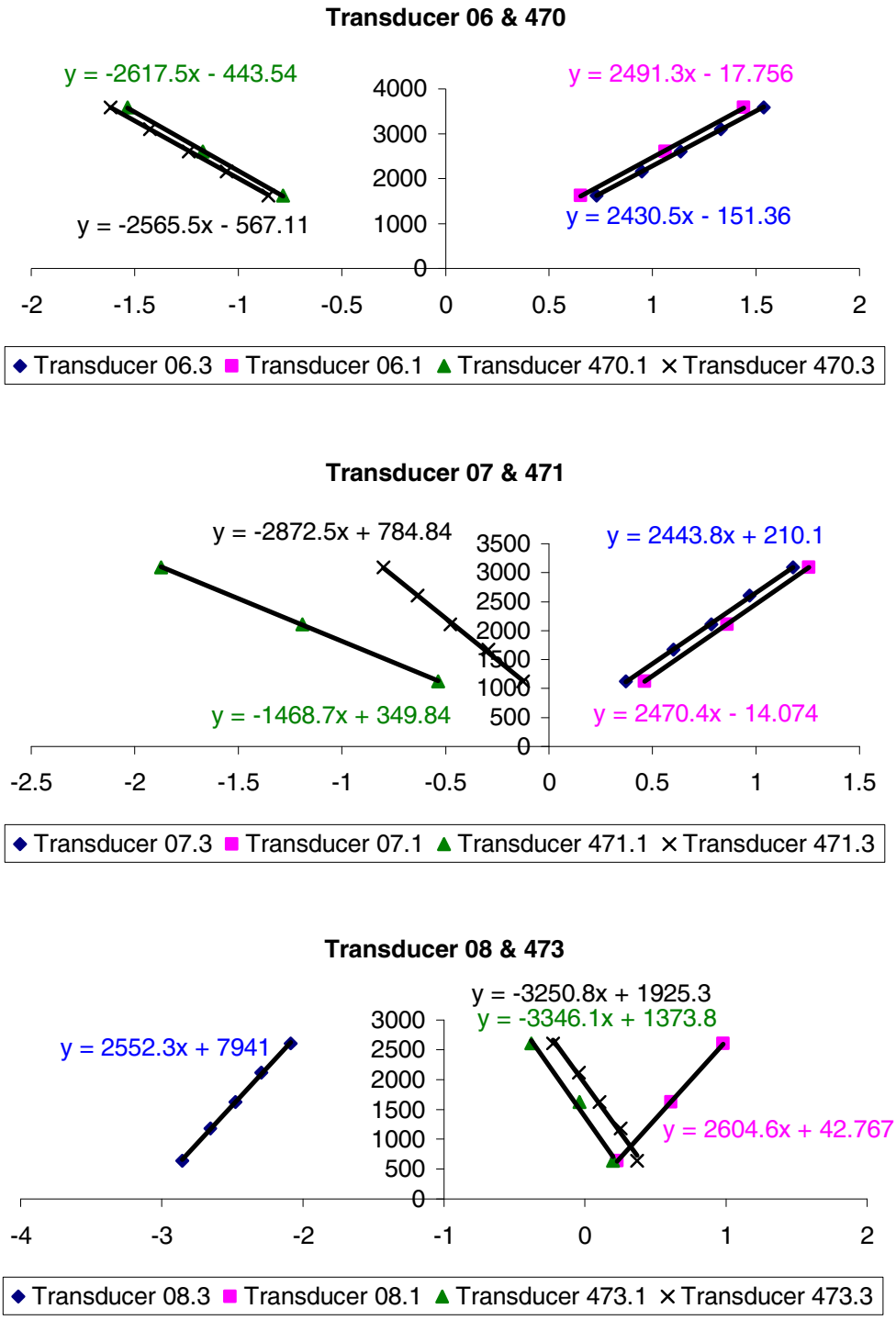

Figure C.20. Calibration functions for pressure transducer row four to six based on calibration one and three (Calibration on transducer 465 and calibration no. 3 is 465.3). Pressure is measured in Pa and voltage in volt (x-axis).

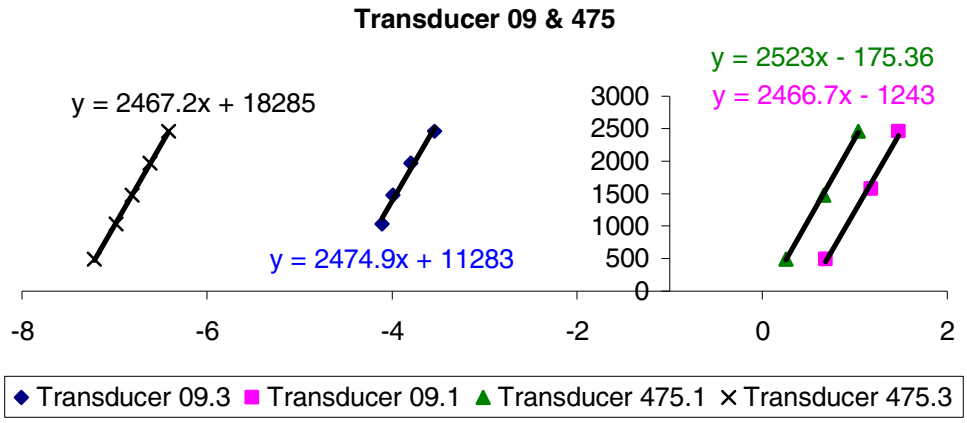

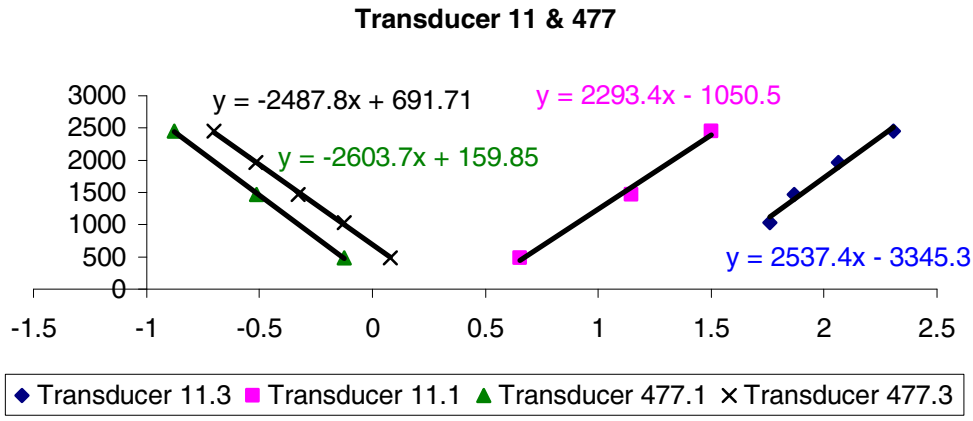

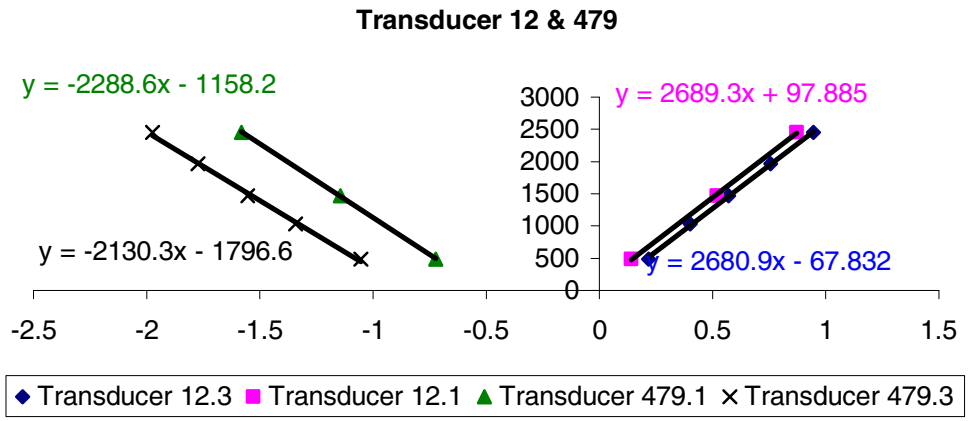

Figure C.21. Calibration functions for pressure transducer row seven and eight based on calibration one and three (Calibration on transducer 465 and calibration no. 3 is 465.3).. Pressure is measured in Pa and voltage in volt (x-axis).

Table C.4. Calibration functions used when converting from voltage to pressure for the 16 pressure transducers in row AA and BB based on Calibration no. 3, the offset b is measured during the sampling. The transducers marked with red have proved unreliable during the calibration.

Elevation [mm]	**Channel**	**Row AA**	**Function** y = a x + b	**Channel**	**Row BB**	**Function** y = a x + b
140	11	02	y = 2121.1 x + b	19	463	y = -2372.3 x + b
285	12	03	y = 1787.7 x + b	20	465	y = -2611 x + b
335	13	06	y = 2430.5 x + b	21	470	y = -2565.5 x + b
385	14	07	y = 2443.8 x + b	22	471	y = -2872.5 x + b
435	15	08	y = 2552.3 x + b	23	473	y = - 3250.8 x + b
450	16	09	y = 2474.9 x + b	24	475	y = 2467.2 x + b
450	17	11	y = 2537.4 x + b	25	477	y = -2487.8 x + b
450	18	12	y = -2130.3 x + b	26	479	y = 2680.9 x + b

C.6 Experiments - input and results

The aim of the experiments was to determine how well the SPH method is to handle 2-D impact problems.

- Experiment no. 1: An experimental study of the variance and correlation of the sampled data
- Experiment no. 2: Train of regular waves rising and hitting the wall and platform with difference in water wave height *H* and period *T*.
- Experiment no. 3: Series of regular waves rising and breaking just before the platform (1-2 metres)

The following is a presentation and processing of the most important results in order to make them ready for a later comparison with the SPH model. The properties of the generated waves are chosen in order to create an impact situation as depicted in Figure C.22.

Figure C.22. The wall and platform depicted just before wave impact (to the left) and during the impact (to the right) during the first series of experiments.

The wave flume and the size of the platform and wall as specified in Section C.4 makes a range of wave height and period available, the lower limit being waves that fail to hit the platform and the upper limits waves that break before they reach

the platform. It is also necessary to complete measurements before reflected waves reach the wall again as it would otherwise be impossible to see the difference between the generated and reflected waves. The range used as input is $1.0 \leq T \leq 2.0$ [s] and $0.15 \leq H \leq 0.25$ [m] and the sample frequency is chosen as 1000 Hz on all channels in order to measure the instantaneous forces in a wave impact.

C.6.1 Experiment no. 1 – Reliability of sampling

The first experiment is conducted to get figures on the reliability of the collected samples. To this end a series of experiments is conducted with the same input i.e. identical movement of the paddle and still water before the initiation of each sample. It is chosen so send a small group of waves with a single wave breaking against the platform. The wave height and period is chosen so that the waves does not break before they reach the end of the flume. Paddle movement, the generated waves and the corresponding pressure measured beneath the platform is depicted in Figure C.23.

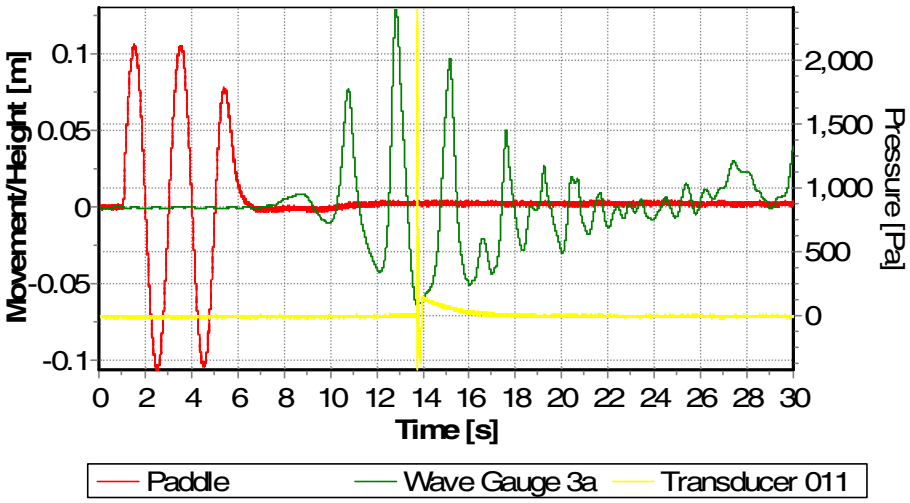

Figure C.23. The movement of the paddle and the generated waves and the corresponding single hit beneath the platform recorded as a spike by transducer 011.

The samples are compared in two ways. A maximum value is measured in each sample when the largest of the generated waves hits the wall and breaks against the platform, cf. Figure C.23. The maximum value of all samples on one channel is compared to determine their reliability when measuring a peak value. Furthermore the entire sample on corresponding channels is compared using cross correlation. *Note that all comparisons in this section are done with the noncalibrated data i.e. all data is presented as volts.*

Experiment input and signal processing

The input is chosen to generate a group of non-breaking waves that hit the platform with a water depth of 0.25 m. The values were also chosen to lie in the same range as the ones used in subsequent experiments in order to allow for comparison, cf. Table C.5.

Table C.5. The input used to generate the waves depicted in Figure C.23 and corresponding measured wave heights after the paddle and before the wall. The wave gauge values are approximated using a time series analyses on the sampled time series.

Paddle input		**Wave gauge group no. 1**			**Wave gauge group no. 3**		
H_{input}	T_{input}	H_{max}	T_{max}	L_{max}	$H_{i,max}$	$T_{i,max}$	L_{max}
[m]	[s]	[m]	[s]	[m]	[m]	[s]	[m]
0.2	2	0.13	1.75	3.75	0.10	2	3.45

The following statistic parameters are calculated: The mean value μ_X (C.2), the standard deviation σ_X (C.3) and the cross correlation ρ_{XY} (C.5) between two time series of pressure measurements sampled on the same transducer. The cross correlation is defined using the cross covariance κ_{XY} (C.4). The cross correlation ρ_{XY} between two series $X(t)$ and $Y(t)$ is calculated where $\{X(t),\ t \in T\},\ T=\{1,2,\ldots,n\}$ and n is the number of samples. [Nielsen, 2000] & [IMSL, 2007]

$$\mu_X = E[X] = \int_{-\infty}^{+\infty} x\, f_X(x)\, dx \tag{C.2}$$

$$\sigma_X^2(t_i) = E\left[\left(X(t_i) - \mu_X(t_i)\right)^2\right] \tag{C.3}$$

$$\kappa_{XY}(t_i, t_j) = E\left[\left(X(t_i) - \mu_X(t_i)\right)\left(Y(t_j) - \mu_Y(t_j)\right)\right] \tag{C.4}$$

$$\rho_{XY}(t_i, t_j) = \frac{\kappa_{XY}(t_i, t_j)}{\sigma_X(t_i)\,\sigma_Y(t_j)} \tag{C.5}$$

where

$E[X]$ is the expected value of the stochastic value X.

As the series have already been aligned in Section C.5.1, the cross correlation between $X(t)$ and $Y(t)$ is calculated using $i = j$. It would have been possible to use the cross correlation to align the series by keeping one index constant and vary the

other thereby finding the combination with highest correlation but a quick test shows that this only makes a small difference in the final cross correlation value.

The variable definition above was given for continuous random variables. When working with the sampled time series the variables are named as follows, cf. Table C.6.

Table C.6. The variable definition used when calculating the reliability of the maximum values and the cross correlation of two different time series.

Maximum values			Time series		
X_{Max}	-	Maximum measured value in all the 27 time series	$R_{c,mean}$	-	Mean cross correlation coefficient of the 27 sampled time series
$X_{max,mean}$	-	Mean of the Maximum measured value in all the 27 time series	s_R	-	Standard deviation of the cross correlation
s_{Max}	-	Standard deviation of maximum values	δ_R	-	Coefficient of variation of the cross correlation
δ_{Max}	-	Coefficient of variation of maximum values			

The standard deviation s, the cross correlation coefficient R_c, the mean value X_{mean}, the max value X_{max} and the coefficient of variation δ given as (C.6).

$$\delta = \frac{s}{X_{Mean}} \tag{C.6}$$

The main result of the measurement of the 16 transducers is presented in Table C.7 and Figure C.24 and used on the next few pages. The presented cross-correlation is a mean value of the 26 possible combinations at each transducer. The sampled series and MatLab files with post processing are available on the CD-ROM and the position of the 16 transducers is depicted in Figure C.10.

Table C.7. The results from experiments no. 1 for the pressure transducers and the paddle, the data is based on 27 sampled time series. The position of the transducers is depicted on Figure C.10.

Transducer	**Paddle**	**002**	**003**	**006**	**007**	**008**	**009**	**011**	**012**
Channel	**10**	**11**	**12**	**13**	**14**	**15**	**16**	**17**	**18**
	[V]	[V]	[V]	[V]	[V]	[V]	[V]	[V]	[V]
X_{Max}	0.000	1.706	1.761	0.895	0.925	4.569	7.372	1.612	0.412
$X_{max,mean}$	0.000	1.566	1.565	0.689	0.663	3.502	6.774	1.518	0.323
s_{Max}	0.000	0.049	0.084	0.083	0.137	0.562	0.367	0.048	0.038
δ_{Max}	0.000	0.031	0.054	0.120	0.207	0.161	0.054	0.031	0.118
$R_{c,mean}$	0.990	0.963	0.977	0.980	0.971	0.963	0.972	0.980	0.949
s_R	0.023	0.032	0.034	0.008	0.007	0.014	0.019	0.005	0.012
δ_R	0.024	0.034	0.035	0.008	0.007	0.015	0.019	0.005	0.013

Transducer	**-**	**463**	**465**	**470**	**471**	**473**	**475**	**477**	**479**
Channel	**-**	**19**	**20**	**21**	**22**	**23**	**24**	**25**	**26**
	-	[V]	[V]	[V]	[V]	[V]	[V]	[V]	[V]
X_{Max}	-	0.964	1.082	0.814	1.317	5.910	9.910	1.179	0.992
$X_{max,mean}$	-	0.900	0.936	0.696	0.982	3.215	5.984	0.928	0.781
s_{Max}	-	0.033	0.053	0.056	0.197	1.150	1.567	0.092	0.088
δ_{Max}	-	0.036	0.057	0.080	0.201	0.358	0.262	0.099	0.112
$R_{c,mean}$	-	0.957	0.973	0.977	0.971	0.938	0.927	0.948	0.321
s_R	-	0.032	0.036	0.017	0.013	0.033	0.077	0.010	0.096
δ_R	-	0.034	0.037	0.017	0.013	0.035	0.083	0.010	0.298

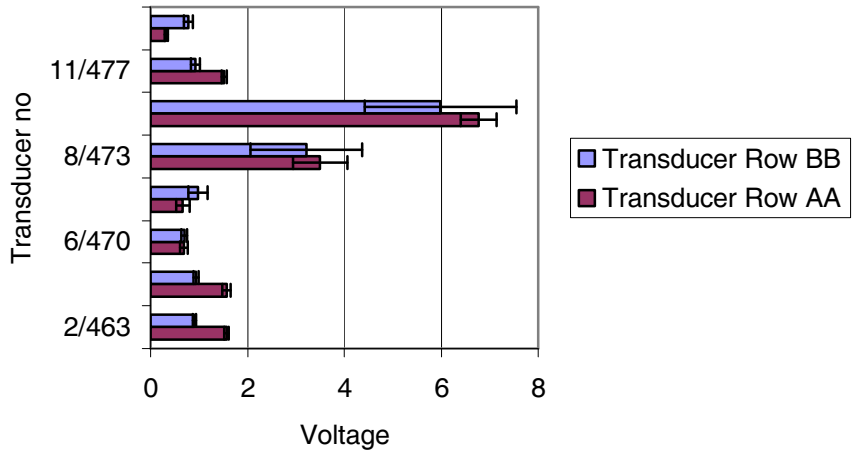

Figure C.24. Mean $X_{max,mean}$ of the maximum values measured on the 16 transducers together with the calculated standard deviation s_{Max}.

Reliability of maximum samples

With the chosen wave period the first wave reaches the wall after approximately 14 seconds. The deviation and mean values of the 30 samples are presented in Table C.7. The depicted cumulative distribution functions in Figure C.25 show that the deviations of all except two transducer positions are comparable in appearance. A closer look on the cumulative distribution of the maximum measurement on 16 pressure transducers is available in Figure C.27.

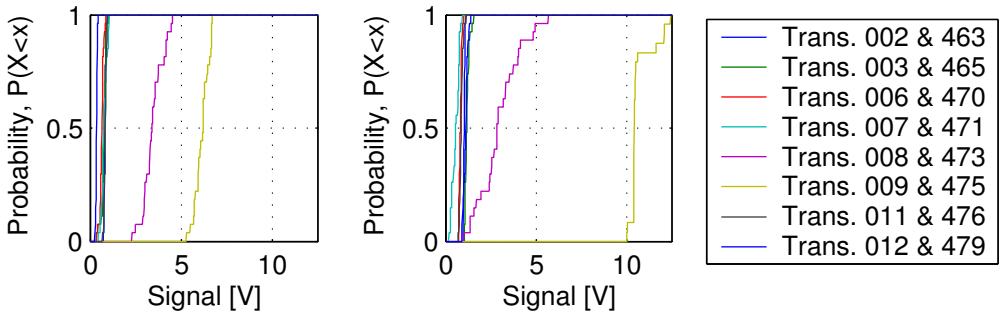

Figure C.25.Cumulative distribution functions of the 16 pressure transducers divided into the two rows. Row AA is to the left and row BB is to the right.

The four transducers 008, 473, 009 and 475 are placed at the bend between wall and platform and they are also the four transducers experiencing the biggest water impact. The agreement between all channels except these four indicate that the sampling frequency has not been big enough to sample what happens at these positions. Another explanation for a high δ could be a low number of samples but as this does not apply for all transducers it is not the case in this experiment. The case is further substantiated by looking at Figure C.26 where two samples of transducer 473 are compared. Here it is evident that the maximum is based only on one measurement.

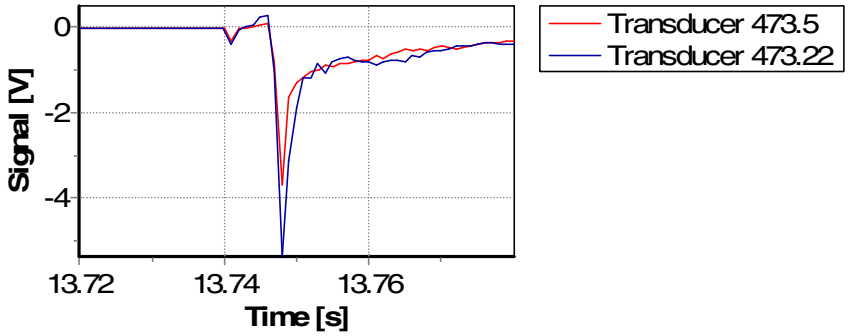

Figure C.26. In this figure, two different maximum samples at transducer 473 are compared to each other. It is evident that the maximum signal is measured in a single time step.

The remaining transducers have relatively small deviations of their maximum samples as evident from Figure C.25. It is therefore concluded that although they may also have benefited from a higher sampling their reliability is acceptable. The Figure C.27 and Figure C.28 show a cumulative distribution of each channel compared to the corresponding normal distribution showing that the sampled data has a normal distribution.

Reliability of the sampled time series

The sampled time series are compared to each other with a cross correlation, R_c, between two samples on the same transducer. The corresponding transducers in row AA and BB are not compared as they are not of the same type. There are a total of 351 combinations between the 27 measured samples. As there is no point in presenting them all in this text, the mean of the samples, $R_{c,mean}$, is computed and presented in Figure C.27, Figure C.28 and Table C.7.

The cross correlation of the sampled channels shows that as a whole there is a good correlation (more than 0.95 on average) between the sampled time series. The only exception is transducer 479 and this is due to a great deal of interference on all the measured channels. It has not been possible to remove this interference with filtering as it is divided on a number of frequencies and no conclusions about the reliability can be made for this transducer. The interference has been removed in subsequent experiments by increasing the amplification. The amplification has also been modified on several other transducers as it was possible to do it and keep within the sample range of WaveLab (±10 V).

The sampled paddle movement was also tested with a cross-correlation analysis and as it is evident from the result of Table C.7 where R is equal to 0.99, this sample is by far the most reliable. With this reliability it is of little importance which of the sampled time series is loaded and used as a base for the computed SPH model.

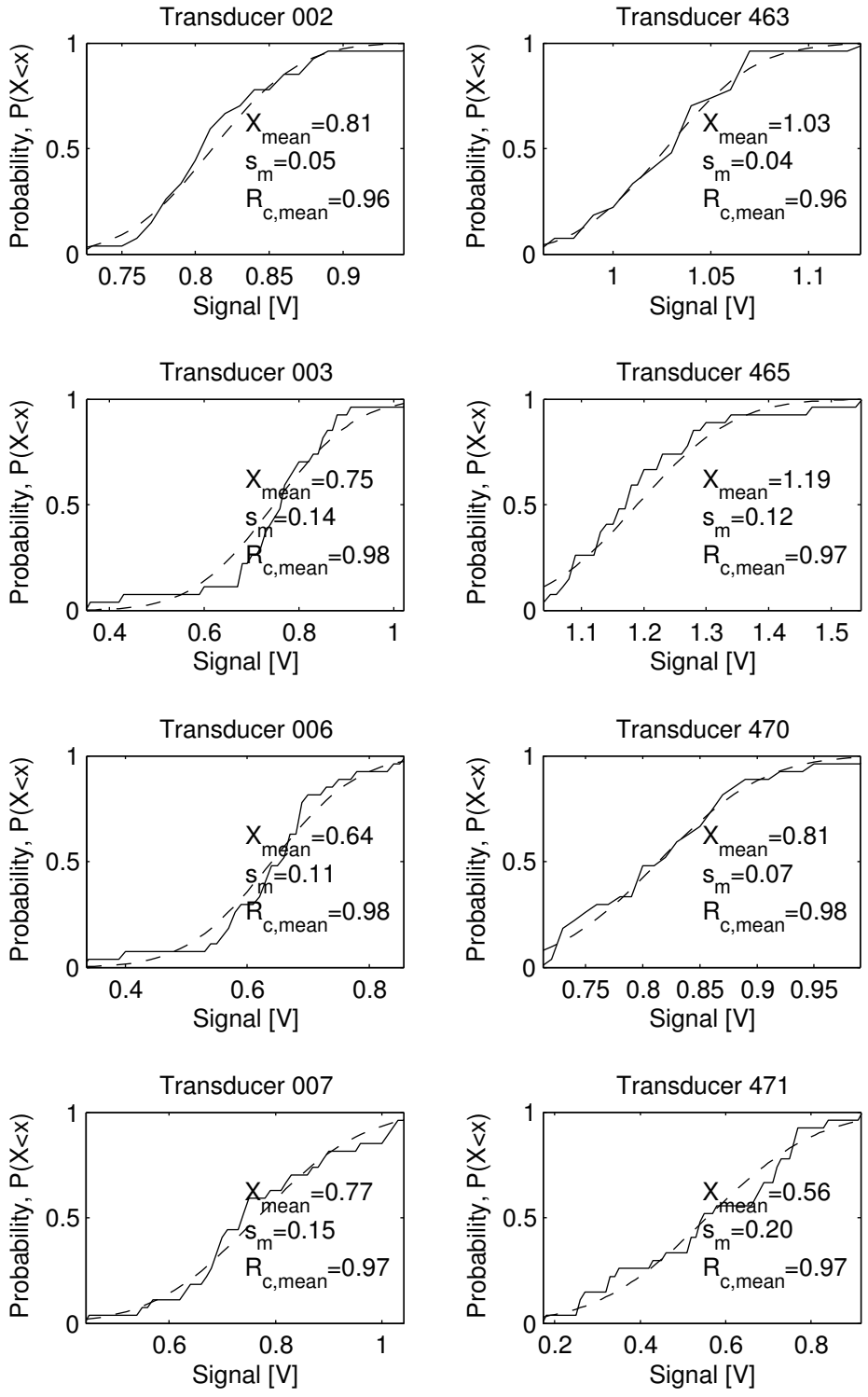

Figure C.27. Sampled cumulative distribution functions (solid) for the first eight transducers compared with a fitted normal distribution (dashed).

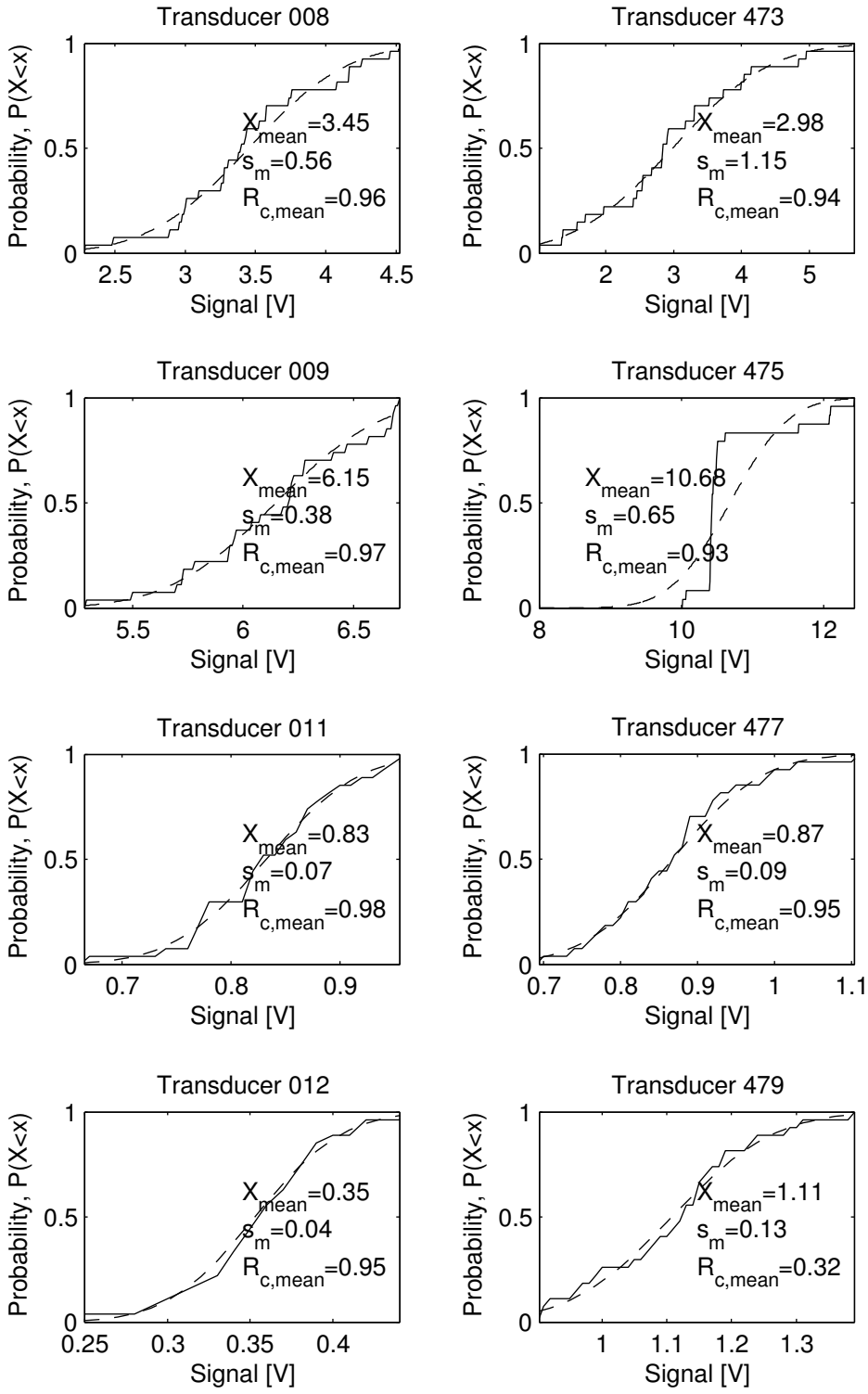

Figure C.28. Sampled cumulative distribution functions (solid) for the first eight transducers compared with a fitted normal distribution (dashed).

Interaction between structure and water

During the first samples it was noted that the transducers measured a lot of high frequency signals during wave impact. It was speculated that these signals were due to vibrations in the structure and that they might have an impact on the measured pressure. To test if this was the case a few samples were run, in which the mass of the experimental setup was changed by placing two concrete bricks on top of the platform as depicted in Figure C.29.

Figure C.29. Two concrete bricks placed on top of the platform in order to significantly chance the eigen vibrations of the structure.

The plots depicted in Figure C.30 compare signals with and without the added mass. The transducer 477 is used for comparison because of its reliability and its position beneath the platform where the wave hits hardest. The plot shows that there are indeed changes in the small fluctuations after the impact when the bricks are added. The plot shows that it has an influence on the maximum measurements as transducer 477.28 (where 28 is the number of the sample) is outside the expected bounds plotted in Figure C.28. The same is the case to a lesser degree with transducer 011 but Figure C.31 indicates that it might not make any difference for neither the maximum measurements nor the time series as a whole.

It is not possible to make flexible boundaries that might be able to model the reaction between the water and the structure with the present version of SPHysics. Therefore the lack of impact must be expected to influence the results especially at the maximum measurements. Work has begun to implement FEM with SPH and then it might be possible to take the flexibility of the structure into consideration [De Vuyst et. al; 2005].

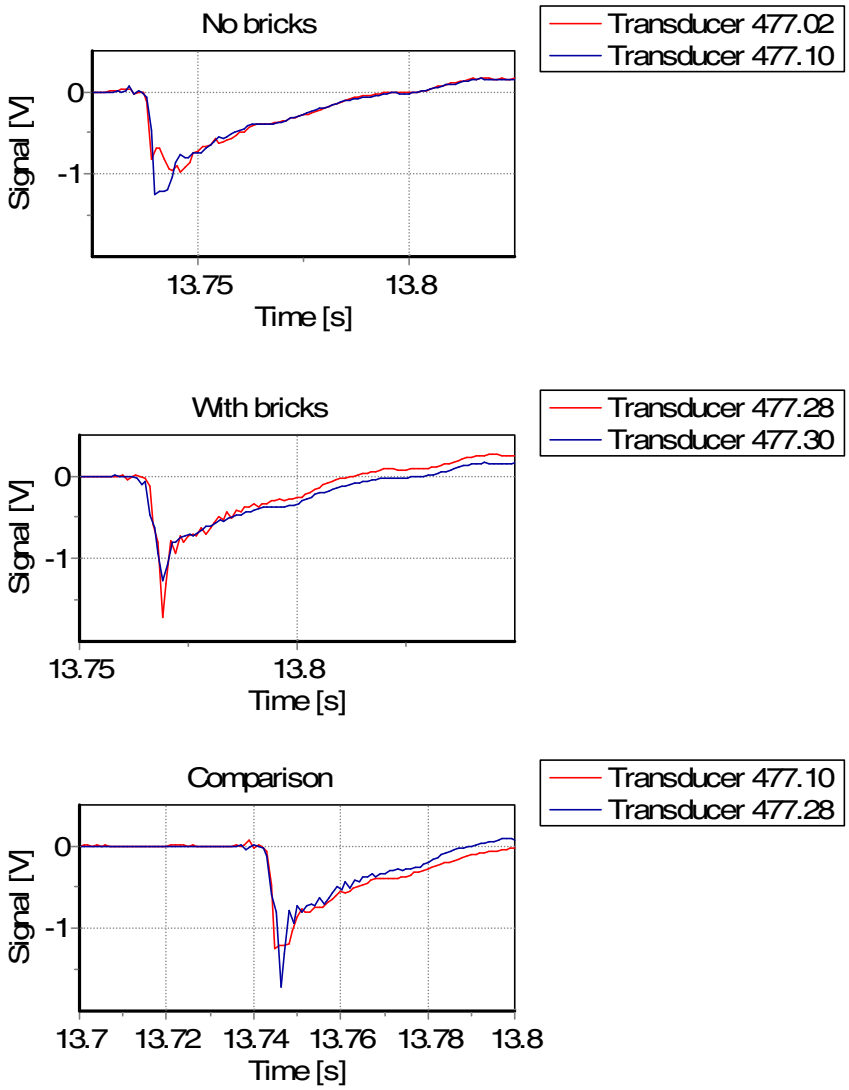

Figure C.30. A comparison of measurements around the maximum of the time series at transducer 477 is depicted on the three plots in this figure.

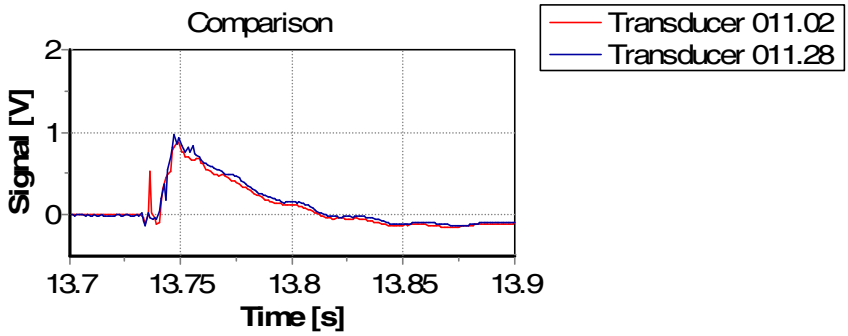

Figure C.31. A comparison of measurements around the maximum of the time series at transducer 011 is depicted on this figure.

C.6.2 Experiment No. 2 - Wave impact

The aim of this second round of experiments was to determine the impact pressure on the structure during a series of regular waves. The experiments were conducted with different combinations of wave properties in order to compare how this influences the force of the impact. The experiment is conducted with a water depth h_{SWL} of 0.25 m just before the foot of pebbles.

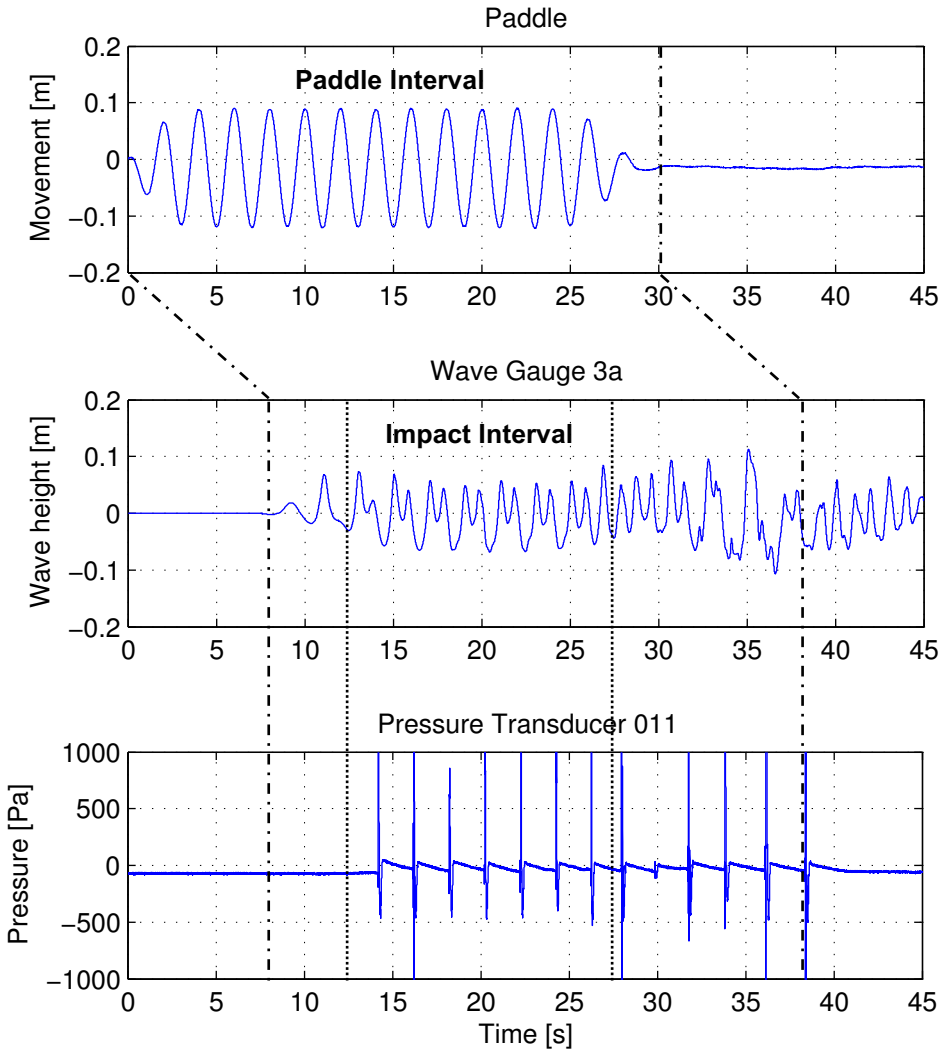

Figure C.32. On this figure the movement of the paddle (Paddle interval) the generated waves and the impact on the platform recorded by pressure transducer 011 and run no. 3 is depicted. Only the approximately 12 seconds of the time series is used (Impact interval) before reflected waves reach the structure.

The paddle movement and an example of the generated waves and the corresponding pressure are depicted in Figure C.32. From the plot it is evident that the train of regular waves generated by the paddle in the "Paddle interval" travels along the 16 m long flumes in approximately nine seconds before the first wave is measured by the Wave Gauge 3a. It follows that the wave speed is approximately 1.8 m/s and it is possible to sample a total of 30 seconds before the reflected wave reach the wall for the second time. This is clearly seen in Figure C.32 where the wave gauges measures a stable mix of incoming and reflected waves until 27 seconds into the sample. The same system is detectable when comparing the measured waves and impact pressure at transducer 011. It follows that with the generated wave properties is the desired part of this sample approximately 12 s $<t<$27 s (impact interval). The situation depicted in Figure C.32 is typical for the experiments No. 2-5. The negative pressure detected by the pressure transducer is discussed further on page 68.

The original intent of the pebble foot depicted in Figure C.3 was to lift the waves in front of the wall and control when and where the waves where supposed to break. But during the initial tests it was discovered that no foot was necessary and that the impact was generated by the combination of incoming and reflected waves, i.e. wave height, period and water depth. The first incoming wave is reflected by the vertical wall and subsequently doubling the height of the next incoming wave. The second waves rises and sucks water away in front of the structure (B), cf. Figure C.33. The second wave then crashes against the structure (C-D) and deflects back into the flume (D), no water is overtopping. This is depicted as a series of pictures in Figure C.33. It was proven impossible to get waves to break closer than 2 meters from the wall even with and enlarged foot.

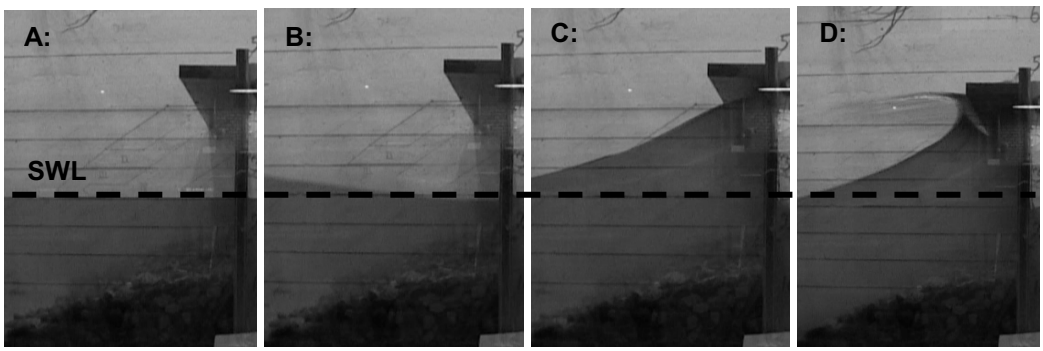

Figure C.33. The impact of the structure depicted in a series of pictures from just before to just after impact. The dotted line shows the original SWL.

A number of runs with different wave properties are conducted and the sampled time series are compared on three different levels to prepare for a later comparison with numerical results.

- The variance of the time series sampled on pressure transducers during the impact time interval. The magnitude of the variance will tell about the energy level of the whole time interval.
- Comparison of wave with different parameters and the sampled pressure during a single impact in the middle of the impact interval.
- A time domain analysis is used on the sampled wave data in order to compare with an analysis on the numerical results at the same positions.

Firstly the samples of a few chosen transducers are compared in order to ensure that measurements do not fluctuate wildly. This shows that the key statistical figures computed in Section C.6.2 are viable and that the equipment is working. The impacts are generated by a series of regular waves. When the waves run in a continues series there is no dissipation and the relation between the mean wave energy E_w (kinetic and potential) during a single period and wave height H is given in equation (C.7).

$$E_w = 1/8\rho g H^2 \tag{C.7}$$

Equation (C.7) counts for linear wave theory but the relation $2H \Rightarrow 4E_w$ is used when choosing the wave properties to get a reasonable relation between the used waves.

Experimental input and signal processing

The input is chosen to generate a series of non-breaking waves that hit the platform with a water depth of 0.25 m. The values were chosen by trial and six time series were chosen for comparison with the numerical results. Three were recorded with the pebble toe in place and three runs were conducted without the pebble toe. The toe is depicted in Figure C.3 and the run is presented in Table C.8.

Table C.8. Input in the wave generator and the generated incoming waves at the three groups of wave gauges found using a time-domain analysis of the sampled wave series (done in WaveLab).

Setup:		**With toe**			**Without toe**		
		Run 1	**Run 2**	**Run 3**	**Run 4**	**Run 5**	**Run 6**
H_{input}	[m]	0.15	0.15	0.2	0.2	0.2	0.25
T_{input}	[s]	1	2	2	1.5	2	2
Impact time	[s]	25<t<40	17<t<27	15<t<25	20<t<30	15<t<25	17<t<27
Group 1:	[s]	10<t<25	7<t<15	5<t<15	7<t<17	5<t<15	7<t<17
H_m	[m]	0.09	0.09	0.12	0.12	0.12	0.15
T_m	[s]	1.00	2.00	2.00	1.50	2.00	2.00
***L* (linear/5th stokes)**	[m]	1.60	4.67	4.70	3.10	4.70	4.70
H^2	[m^2]	0.008	0.008	0.014	0.014	0.014	0.023
Group 2:	[s]	15<t<25	10<t<20	7<t<17	10<t<20	7<t<17	9<t<17
H_m	[m]	0.08	0.08	0.11	0.11	0.11	0.13
T_m	[s]	1.00	2.00	2.00	1.51	2.00	2.00
Group 3:	[s]	27<t<37	15<t<27	15<t<25	20<t<30	15<t<25	17<t<27
H_m	[m]	0.09	0.10	0.13	0.14	0.14	0.17
T_m	[s]	1.00	2.01	1.99	1.48	2.00	2.00

The runs in Table C.8 represent the chosen selection of wave properties. The selection was limited by the geometry of the flume, the chosen water depth and the size of the structure. The period interval ($1 \leq T_{input} \leq 2$) is chosen as the longer periods would generate waves too long to fit within the flume and waves with shorter periods would break before reaching the structure. The wave height interval ($0.15 \leq H_{input} \leq 0.25$) was chosen to fit the period interval and generate waves that impact on the platform and do not break before reaching the wall. The wave length L from Table C.8 is based on measured waves with a water depth of 0.7 m. The length would off course decrease slightly as the waves reach shallow water at the end of the flumes, cf. Figure C.10.

Table C.9. The variance σ_{Impact} of the six experimental runs computed in the impact time interval given in Table C.8. The interval is chosen based on the amount of time. Only regular waves generated by the paddle reach the wall. The position of the transducer rows is depicted on Figure C.10

	Transducer	**002 /463** $\cdot 10^5$	**003 /465** $\cdot 10^5$	**006 /470** $\cdot 10^5$	**007 /471** $\cdot 10^5$	**008 /473** $\cdot 10^5$	**009 /475** $\cdot 10^5$	**011 /477** $\cdot 10^5$	**012 /479** $\cdot 10^5$
Run 1	Row AA	0.40	0.04	0.00	0.00	-	-	-	-
	Row BB	0.48	0.28	0.04	0.01	-	-	-	-
Run 2	Row AA	2.63	0.37	0.14	0.02	-	-	-	-
	Row BB	3.28	1.08	0.21	0.08	-	-	-	-
Run 3	Row AA	17.32	2.76	1.74	0.81	3.22	5.42	1.60	0.20
	Row BB	21.64	7.22	2.26	1.42	5.24	5.71	1.46	1.48
Run 4	Row AA	8.79	1.02	0.44	0.06	0.03	0.05	0.01	0.00
	Row BB	10.94	2.75	0.74	0.19	0.20	0.22	0.01	0.57
Run 5	Row AA	11.37	1.83	1.22	0.61	2.17	4.44	1.00	0.20
	Row BB	13.99	4.75	1.47	1.08	4.43	4.96	1.74	0.53
Run 6	Row AA	15.13	3.03	2.97	2.69	7.19	11.20	5.79	1.92
	Row BB	18.65	7.33	3.38	4.11	13.05	13.03	8.34	7.68

The computed variance of the measurement on the 16 transducers is presented in Table C.9 and used on the next few pages. The presented results are the mean value of the three sampled time series with identical wave properties. The sampled series and MatLab files with post processing are available on the CD-ROM.

Wave measurements

Waves are measured at three different positions in the channel as it is depicted in Figure C.8. The measured wave at each group of gauges is listed in Table C.8 and an example is depicted in Figure C.34 based on Run no. 5. The depicted wave measurements show how the waves travel the flume and show when the first reflected waves reach the gauges. It is possible to perform a time domain analysis on the incoming regular waves at wave gauge 1c and 2c but at wave gauge 3c it is necessary to perform a reflection analysis to incoming and outgoing waves. The picture repeats itself for the remaining runs. A rough estimate of the time it takes before the waves reach the flume for the second time is available by combining the wave properties of wavelength and period in Table C.8.

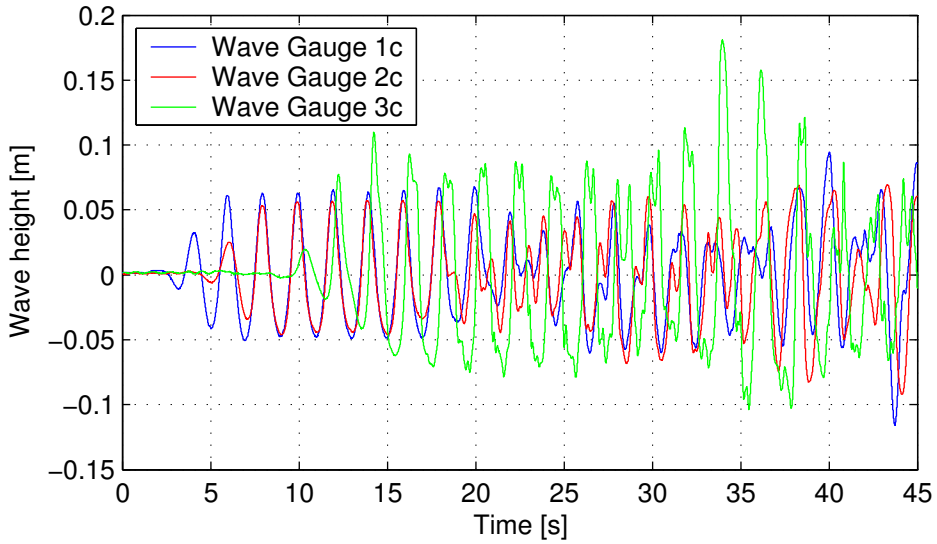

Figure C.34. Run no. 5 is used as example of the wave measurements at the three groups of gauges in the wave flume.

Impact interval – Energy level

The energy levels of the measured time series are compared by plotting the computed variance presented in Table C.9. The two rows of transducers AA and BB are depicted in Figure C.35 and Figure C.36 respectively.

The comparison of the individual transducers shows that they agree about the general trend of a wave impact on the selected structure. The Runs with the same wave properties are equal in size the difference being at transducer 002/463 where the absence of a pebble foot makes the difference. Also there is a difference between the measurement depending on the type of transducer (Row AA or BB) but this might be due to the uncertainties discussed in Section C.6.1.

The waves of Run no. 1 and 2 are not high enough to create any significant impact and are thus excluded. It is clear from comparing the variance of Run no. 4 and 5 that it is the combination of wave height and period that makes the difference when creating the impact, as only a small change in the wave period removes the impact. That this does not affect the submerged transducers is clear in Figure C.35 the submerged transducers (002-007 & 463-471) are equal in magnitude because Run no. 4 and 5 have the same wave height.

The greatest energy level is measured at the intersection wall and the platform (008-011 & 473-477) and below the SWL (002 & 463). The high variance below SWL is caused by the continuous change in water level due to the waves. The high level of energy at the intersection was foreseeable after conducting the statis-

tical tests in Section C.6.1 as the transducers near the intersection had by far the highest peak readings. This corner is the part of the structure where the force of the impact is measured, the other transducers only measure the water on its way to and from the impact.

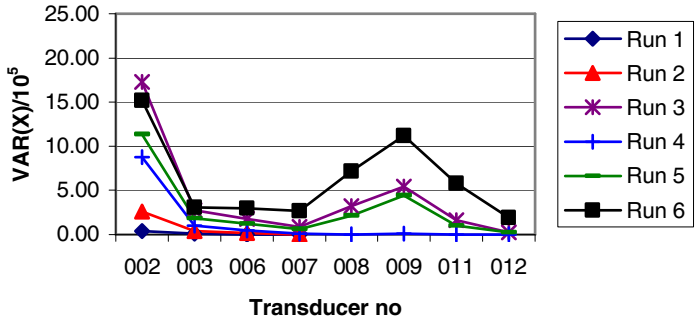

Figure C.35. This is the variance of the measurement on transducer row AA.

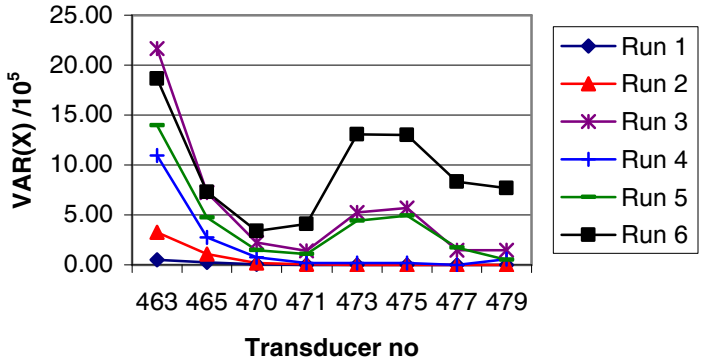

Figure C.36. This is the variance of the measurement on transducer row BB.

Single impact

The single impact is based on a comparison between run no. 5 and 6 as they have the same period but two different initial wave heights, cf. Table C.8. The two runs are compared by plotting the third impact in each series the result is depicted in Figure C.37 and Figure C.38. It is evident from the depicted impacts that the impact on the structure hits all the transducers within a few 1/10 of a second. The two rows of transducers show roughly the same impact history with the largest difference being the peak pressure around transducer no. 15-17 and 473-477. The two different runs also show that not only the maximum pressure but also the duration of this maximum changes when generating higher waves.

The comparison is between time series that each represents a single run. The reliability study of Section C.6.1 (Table C.7) show that there is a high level of correlation between two time series measured with the same parameters. This shows that a direct comparison between two time series is possible.

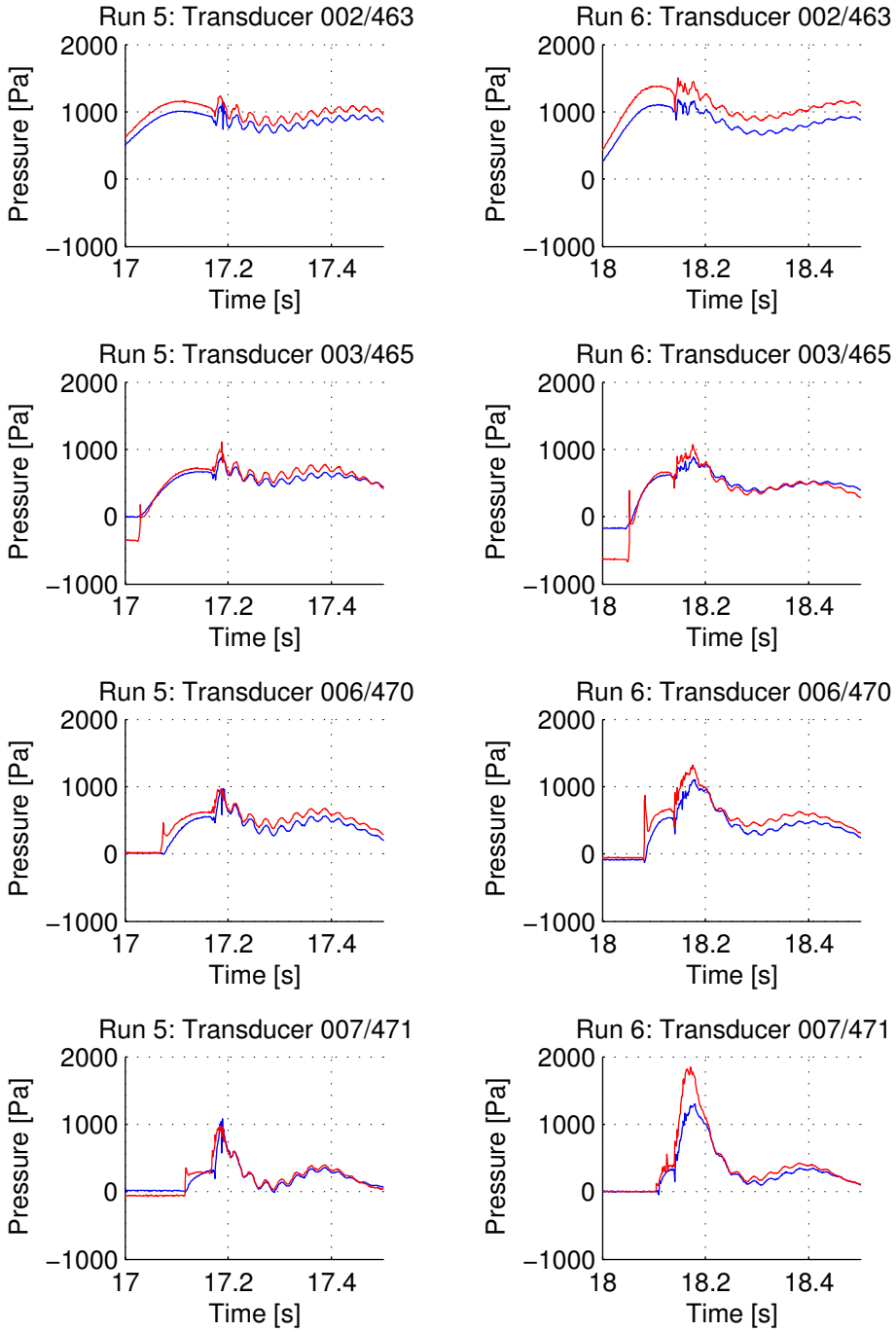

Figure C.37. The first four levels of transducers from 002-007 and 463-471. In each run is row AA (blue) and row BB (red) depicted. The position of the transducers is depicted on Figure C.10.

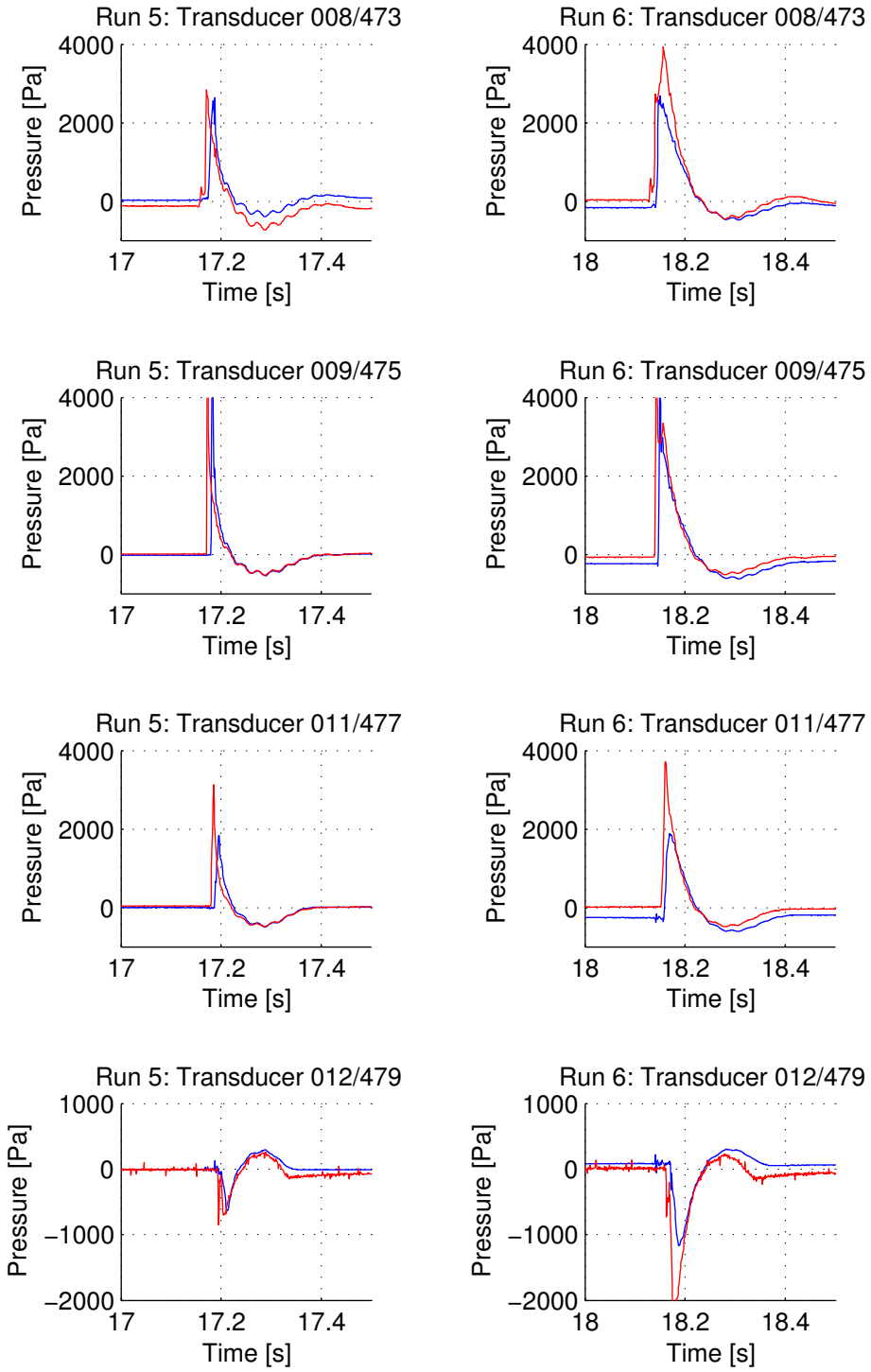

Figure C.38. The first four levels of transducers from 008-012 and 473-479. In each run is row AA (blue) and row BB (red) depicted. The position of the transducers is depicted on Figure C.10.

Negative pressure

The measured pressure at transducer 002 depicted in Figure C.32 has positive and negative fluctuations. The transducer is placed above SWL and it is expected that an impact will lead to a measurement of positive pressure. The fluctuations in both directions are however many times larger in a few impacts each sample as depicted in Figure C.39. To study the problem further transducer 003 and 011 are depicted in Figure C.39. They are both placed above still water level and of the same type (Ø8 or Ø19) but only transducer 002 measures pressure significantly smaller than the atmospheric pressure. Studies of the results show that all transducers above transducer 007 and 471 measure this negative pressure at some impacts and two transducers above and two below the line is compared in Figure C.40.

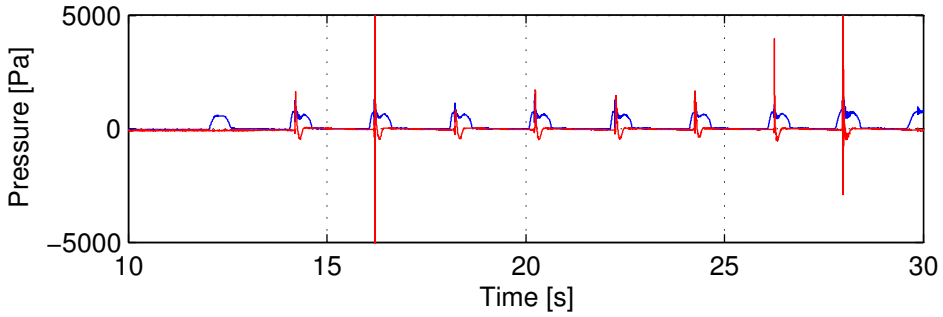

Figure C.39. Comparison between transducer no. 003 (blue) and 011 (red) it shows that only a transducer above a certain level is subject to negative pressure.

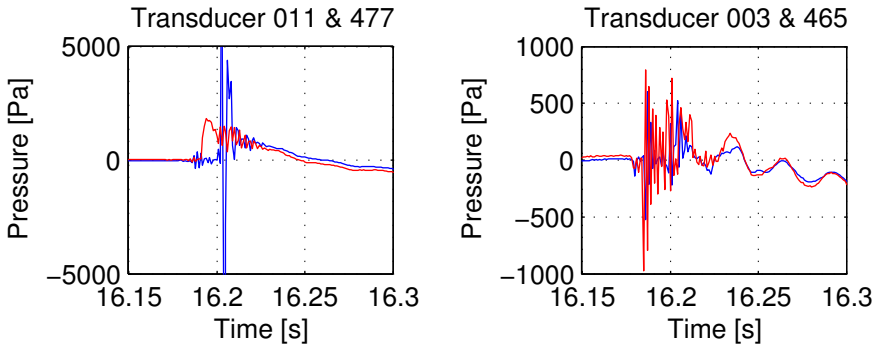

Figure C.40. Comparison between different transducer types at the same level. To the left is transducer no. 011 (blue) and 477 (red). To the right is transducer no. 003 (blue) and 465 (red).

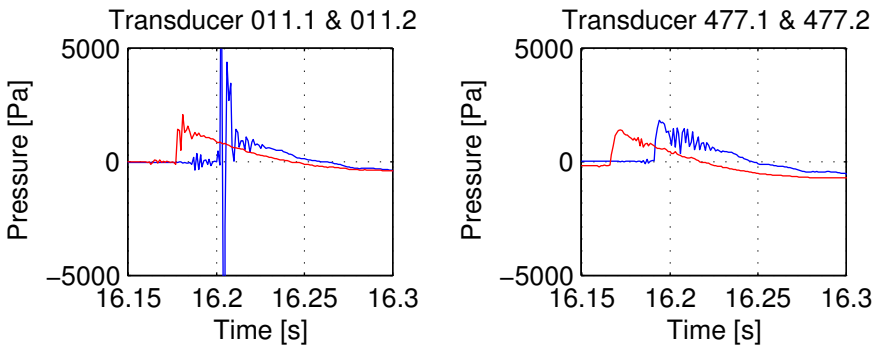

Figure C.41. Plotted comparison between transducer measurements of the same type at the same level but from two different sampled time series 1 (blue) and 2 (red).

The comparison depicted in Figure C.40 shows that for a single impact there is a difference between the measurements of the transducer types Ø8 and Ø19 in the same sample. This is due to some instantaneous effect that is not necessarily present at the transducer in each sample rather than being a fault in the equipment. This is proved by Figure C.41 where new measurements at transducer no. 002 hardly have any fluctuations at all and are similar to the corresponding measurement at transducer no. 477. To further study this phenomenon more than two rows of transducers across the flume would be necessary to substantiate that it takes place at some point of the three dimensional structure.

It is speculated that the high fluctuations in pressure is due to the pressure in confined air between the impacting water and the structure. The confined air would subject to positive pressure during the first part of the impact and negative pressure as the wave disappear again. The negative pressure is due to the confined air expanding when the water recedes trying to fill the enclosure. This effect is instantaneous and not limited to work in only 2D furthermore will the peak value almost certainly differ between two impacts as it is evident in Figure C.39. But it is also evident from the comparison of two different samples in Figure C.41 that the peak values of the same impact are changing. Although the comparisons also show that the overall fluctuations are similar in size and shape. It is not possible to compute this effect with the present version of SPHysics and this must be taken into account when comparing experimental and computational results.

C.6.3 Experiment no. 3 - Breaking waves

The original reason to use SPH was its ability to model a free surface. Each particle represents a volume of water ΔV depending on the smoothing length i.e. the discretization. This will have an effect on when the waves are breaking. Experiment no. 3 was designed to test the impact of breaking waves and more importantly when they break in the flume. The breaking waves in the flume are generated by choosing a wave height of 0.2 m like in Experiment no. 2 but changing the period to only 1 sec. The SWL level before the structure is 0.25 m. The experiment may be compared to the numerical results by comparing measured and computed waves before and after breaking. Furthermore the location of the first breaking waves in the experiment is recorded.

Experiment input and results

With the chosen combination of wave height and period listed in Table C.10 the waves break twice before reaching the wall. The two break points are shown as a sketch in Figure C.42. It was not possible to take real time pictures of the breaking waves due to the layout of the flume.

Table C.10. The input used to generate the breaking waves and the mean measured wave heights/periods at the three groups of wave gauges found with a time domain analysis (WaveLab).

Input		**Group 1**			**Group 2**		**Goup 3**			
H_{input}	T_{input}	H_m	T_m	L	H_m	T_m	$H_{m,incoming}$	$T_{m,incoming}$	$H_{m,reflected}$	$T_{m,reflected}$
[m]	[s]	[m]	[s]	[m]	[m]	[s]	[m]	[s]	[m]	[s]
0.25	1	0.15	1	4.00	0.12	1	0.12	1.02	0.08	1.02

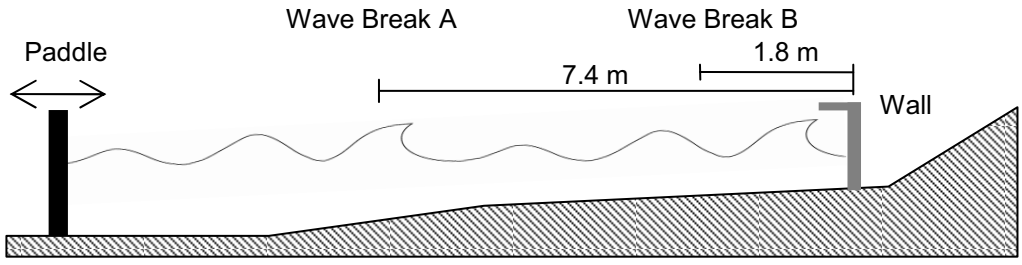

Figure C.42. The waves break twice when travelling the flume depicted on this figure as Break A and B. The location of the first wave breaking is measured from the front of the wall.

The second group of wave gauges is placed 10 m from the wall and the second group is 2 m from the wall. It is evident from a comparison of two wave series measured at group 1 and group 2 that the wave height drops significantly where it should have risen due to shoaling, cf. Table C.10 and Figure C.43. It is not possible to trace the second break as it happens right on top of the last group of wave gauges Figure C.8 and Figure C.43. The location of break A and B was found by running several experiments with the chosen conditions and marking the point where the crest of the wave starts to form. The distances in Figure C.42 are the mean of these observations.

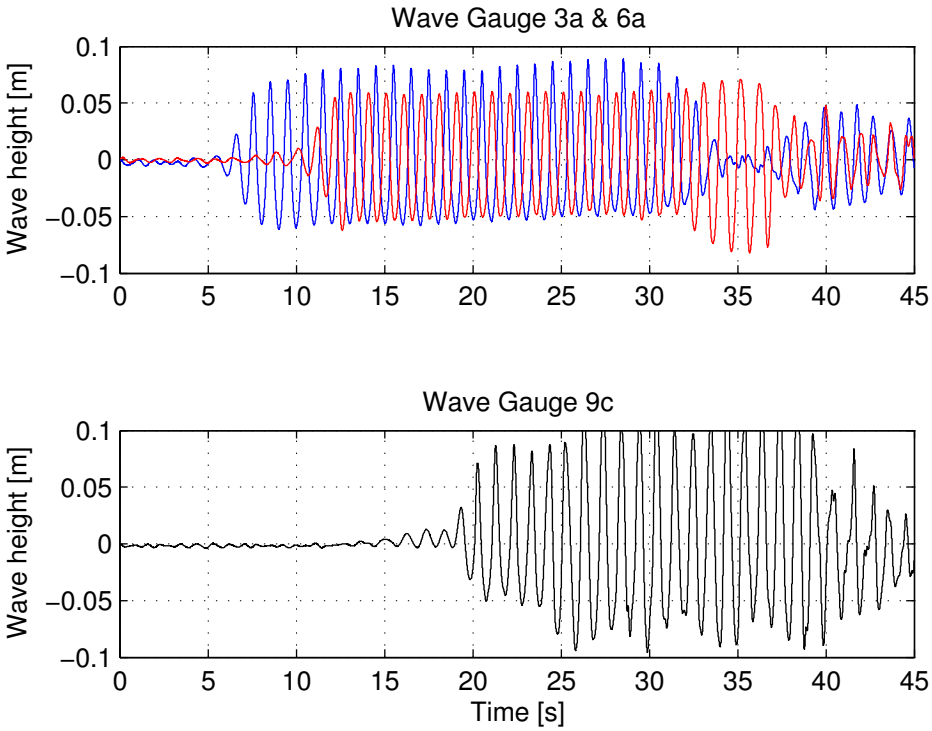

Figure C.43. The measured waves at the wave gauges when waves are breaking in the flume the measurement is compared to waves with a similar period T=1sec but different height from Experiment two and Run no. 1.

C.6.4 Reliability and sources of error

In the following the reliability of the experiments and possible sources of errors is discussed based on the result in the three presented experiments. Generally errors have proven to come from three sources: Inaccurate equipment, erroneous sampling parameters and the post processing.

Reliability

From Experiment no. 2 described in Section C.6.2 it is known that the measured impacts have a high degree of correlation (> 0.90) when the measured time series are compared. The sampled paddle movement has the highest cross correlation equal to one for two generated time series with the same wave properties, cf. Table C.7. The reliability is reasonable high when comparing the maximum of each sample with a coefficient of variance $0.03<\delta<0.12$ for most pressure transducers. The exception is the transducers placed in the intersection between wall and platform. It is clear from the cumulative distribution of Figure C.25 that the reliability of a single sample from these transducers is small with $0.05<\delta<0.36$, cf. Table C.7. The reason for this greater value of δ is probably the chosen sampling frequency of 1000 Hz as the probability of all six transducers (007-009 & 471-475) being wrong is small and closer studies of the sampled peak values show that for some time series the maximum is single highest recorded value i.e. one data point. On the other hand the sampling frequency is adequate to track the peak pressures at the remaining transducers and general history of an impact, cf. Figure C.37.

Sources of error

Having concluded that a single measured time series will not deviate much from the mean it is possible to compare the computed numerical samples with a single experimental counterpart and expect correlation. One has of course to include the other sources of error that will be present with the chosen setup of the experiment. Some vibrations of the structure have been shown to be of little importance, page 57, while others might be off greater significance. Any geometrical errors like deformation of the pebble foot, small movements of the structure and water movement still lingering from previous experiment are measured with Experiment no. 1, Section C.6.1. Other sources of error are listed below.

It is evident from description of the calibration of pressure transducers in Section C.5.3 that although the conclusion is to trust the majority of the transducers, cf. Table C.4, some amount of error will be present when using them for measurements. First of all because of their tendency to shift offset over time and secondly because the maximum measured pressure during the calibration is approximately 5,000 Pa. With a maximum measurement in some samples close to 15,000 Pa it is not certain that the chosen calibration function is still valid. During the post processing of the samples the time series is aligned and zero volts is chosen. As the base level this procedure is not perfect as it is seen from Figure C.37 and Figure C.38. It was chosen to accept these errors in the post processing as greater accuracy would have consumed too much time. These errors must be taken into account when comparing the numerical and experimental results.

The experimental setup has been designed to study a 2-D situation in a wave flume but due to local effects studied in Section C.6.2 there is sometimes great difference between the peak values of two impact. It is speculated that this is due to trapped air introducing a 3-D problem with air trying to escape somewhere along the wall. Nothing can be done about this with the chosen setup although it seems to have the highest level of effect on the peak measurement and the transducers in Row AA. It should not be possible to track this effect when comparing the numerical and experimental results due to the lack of air particles in the SPH model.

It follows from the high correlation between the sampled time series of paddle movement and wave impact that the generated wave series also have a high correlation. The problems with using the chosen type of wave gauges and what is done to minimize errors is described in Section C.4.4. The post processing of the time series sampled on the wave gauges is another matter. There are only a limited number of waves available for a time domain analysis which might be a problem with reflection analysis. On the other hand wave elevations sampled from the numerical model would have the same limits.

The amplification of the transducers has been discussed earlier. When choosing a low amplification the interference from other sources will weigh more in the measured time series. It was initially discovered that especially the transducers of the type Ø8 were sensitive to interference from outside sources and that the highest output of interference originated from the power supply of the laptop used for data sampling. Unplugging the laptop removed a significant part of the interference and it was speculated whether it would be worth the effort to remove the rest. A frequency domain analysis of the sampled time series showed that the remaining interference was evenly distributed at 50, 100, 150 etc. Hz indicating that its origin was electrical. In the end it was decided that the interference was of small significance to final results as it would always be smaller than the maximum sampled values and the figures presented in Section C.6.2 show that it also compared to the remaining readings was limited in size. Trying to use a filter to remove it would only introduce more error than it removed.

C.7 Conclusion on experiments

The purpose of the experiments was to get a source of reference when using the program SPHysics F95 to compute a virtual wave flume. The measured data is divided into to groups: Wave gauge measurement and Transducer impact measurements.

The wave gauge measurements have only been briefly presented during this experiment description but they are important as they describe the wave picture in the flume and will show if the virtual wave flume is able to generate the kinematics of a breaking and non breaking wave. Especially if the wave breaks at the same point as measured in the flume and how much energy i.e. wave height the wave will loose shows the quality of the numerical solution. With the sampled time series there is more than enough data to choose from.

The wave impact on a vertical structure is instantaneous and the occurrence of an impact depends on the properties of the incoming wave and the water level. The experiment was efficient when is came to generating these impact waves and showed that there is a number of things that was not taken into consideration when the experiment was devised. The pebble foot for instance proved to be a disappointment as it was never large enough to interact with the waves until just before they reached the wall. Furthermore the simplification of the problem into 2D created limits for the choice of wave properties.

The results nevertheless show that the experiments were an overall success and useful for comparison with the numerical models and that the sampled time series are reliable. Although one has to take the difference between model and experiment into consideration in any conclusion as arbitrary effects like trapped air proved to have a decisive impact on the results.

The high number of measuring channels generated a vast amount of data for post processing most of which is available on the CD-Rom attached to this report. This proved an asset when looking at the history of an impact and validating the readings as it was possible to get readings from the whole structure. They will not all be used for numerical comparison as only a limited number of computers are available. The Run no. 3, 5 and 6 in Experiment No. 2 and Experiment No. 3 are deemed the most interesting to compare with numerical results due to the presence of and impact against the platform and diversity in wave heights and the experimental geometry.